





Research Article

Traffic Safety Optimization Strategy of Mountainous Highway Tunnel Based on GA-SVR Visual Load Model

Hao Lu ¹, Ting Shang ², Jie Bao ¹ and Ye Liang ²

¹School of Economics & Management, Chongqing Jiaotong University, Chongqing 400074, China

²School of Traffic & Transportation, Chongqing Jiaotong University, Chongqing 400074, China

Correspondence should be addressed to Ting Shang; shangting@cqjtu.edu.cn

Received 2 June 2022; Revised 27 July 2022; Accepted 2 August 2022; Published 14 September 2022

Academic Editor: Yanyong Guo

Copyright © 2022 Hao Lu et al. This is an open access article distributed under the Creative Commons Attribution License, which permits unrestricted use, distribution, and reproduction in any medium, provided the original work is properly cited.

Improving the driving safety of mountainous highway tunnels has become an urgent problem in China, while the existing literature pays more attention to the safety of urban tunnels. From the perspective of visual load, this paper built a GA-SVR model to analyze the influences of speed, design brightness, measured brightness, and position in the Gaogu long tunnel. The results show the following: firstly, the changes of MTPA in the long mountainous highway tunnels can be divided into five stages, which is different from the three-stage division of urban tunnels; secondly, the influencing degree of factors was varied in different stages: the position factor mattered most in stages 1, 2, 4, and 5, while the design brightness had the greatest impact in stage 3; thirdly, the driver's psychological pressure was greatest on the entrance and exit section of the tunnel; lastly, the increased length of mountainous highway tunnels and the long-term enclosed driving environment made the psychological load of drivers intensified. Therefore, it was necessary for the mountainous highway tunnels to consider more accurate gradual lighting design in the 200-m sections after the entrance and before the exit, meanwhile enhancing traffic safety management and protections in the middle of the tunnel.

1. Introduction

In compliance with the national strategy for west China development, more and more highways are being constructed and completed in the western mountainous and hilly areas. Despite such advantages of saving land and shortened travel distance, more accidents with major consequences occur on the mountainous highway. For example, a traffic accident that occurred in the Yanhou tunnel in 2014 caused the death of 40 people and injured 12 people, and another tunnel accident that occurred in Hachihonmatsu tunnel in Japan in 2016 caused the death of 2 people and the injured 70 people. The mountainous highway tunnel is an especially accident-prone section. In Norwegian, the accident rate at the entrance section of the tunnel is 63.7%. In China, the accident rate at the entrance section of the mountainous highway tunnel is more than 50%. According to the Ministry of Transport statistics bulletin, by the year 2020 China had 21,316 road tunnels in total length of 21,993

million meters, which is the largest number in the world [1]. Therefore, how to improve the driving safety of mountainous road tunnels becomes an urgent problem to be solved.

Existing literature have aimed at the urban tunnels with a focus on the influence on driver's safety caused by measured brightness change. The sharp change of measured brightness at portals makes it difficult for the drivers to adapt themselves to the alternation between daylight and shade, which is the main cause of accidents at tunnel portals. However, few existing recorded researches have ever studied the safety of long tunnels on mountain highways. In fact, the long mountain highway tunnel has the following particularity: first, compared with plain highways, mountainous highways have lower speed limits. Due to the small radius and steep slope, the lower value of the horizontal and vertical alignment index of mountain highways and small radius and steep slope often appear. Second, compared with urban tunnels, mountainous highway tunnels are quite different in

cross-sectional form, lighting, ventilation, speed limit, traffic composition, which indicate higher speed, more trucks, and weaker lighting. Third, compared with medium and short tunnels, long tunnels have quite different in lighting, viewing distance, and viewing zone. So, the driver's visual load is more significant, and the viewing distance is shorter [2]. When driving in a long tunnel on a mountain highway, the driver will experience the alteration of "black hole" and "white hole" effects after driving longer and in more extended space. The cumulative superposition effect would cause an excessive visual load on the driver, leading to uncontrolled operation. Therefore, traffic safety in the long tunnel of mountain highway is endangered.

The contributions of this paper are as follows: First, the GA-SVR model simulating the influence of speed, design brightness, measured brightness and position on MTPA (Maximum Transient velocity of Pupil Area) is constructed, and the influences on driving safety in long tunnels of mountain highways are discussed. Compared with the traditional cross-search method and network search method, GA can optimize the parameters in the SVR model and increase the accuracy rate from 89% to 96%. Second, according to the changing characteristics of MTPA, this article divides the mountainous highway long tunnel into five stages for discussion. This division method is different from the traditional three-stage division of urban tunnels. Third, the four influencing factors of speed, design brightness, measured brightness, and position in different stages are compared. The results show that the position has the most significant influence in stage 1, stage 2, stage 4, and stage 5, and the design brightness has the greatest influence in stage 3. Fourth, this study found that the driver's greatest psychological stress stages are stage 2, from the entrance to 200 m after the entrance, and stage 4, from 200 m before the exit to the exit. It is pointed out that it is necessary to consider a more refined gradual lighting design in stage 2 and stage 4. The starting position and set length of the gradual lighting section should be considered in stage 4.

The paper continues as follows: Section 2 provides the literature review; Section 3 describes the experiment method; Section 4 shows the results; Section 5 describes the discussion, and Section 6 concludes the part.

2. Related Research

2.1. Traffic Safety of the Tunnel. The literature on tunnel traffic safety mainly focuses on the influence of new equipment on vehicle traffic safety and tunnel safety design. Vashitz evaluated the effect of on-board display on highway tunnel traffic safety, and the results show that the vehicular display on the degree of distracted drivers is relatively small and does not affect driving safety [3]. Wu analyzed the hydrogen fuel cars that may occur in the highway tunnel fire scenario and fire hazard, and on this basis, discussed the existing tunnel fire safety measures and the improving method of the ventilation system [4]. Chatzimichailidou introduced risk situational awareness methods into the highway tunnel safety field to test the RiskSOAP rationality and applicability of infrastructure and found that the road

tunnel design and maintenance are still needed to strengthen the safety of the space [5]. Hou established China's relevant random parameters of highway tunnel negative binomial model, and the results showed that the proportion of traffic volume, length of the tunnel, heavy trucks, curvature, and pavement rutting are associated with a higher traffic accident frequency, and the distance from the tunnel wall, the distance of adjacent tunnel distance, distress, the international roughness index, coefficient of friction are associated with lower collision frequency [6]. Zhao showed that setting the tunnel retro-reflective arch spacing to 300 m in a curved segment and in the tunnel overall is the best option. In the middle segment, the ideal setting spacing should be 400 m [7].

Existing literature focuses on the use of new communication means and technology to improve tunnel safety design, but from the psychological perspective of drivers, the discussion of tunnel traffic safety is rarely mentioned. In fact, mountain highway tunnels have serious traffic safety risks. Therefore, it is necessary to study the physiological changes of long tunnels on drivers and its impact on traffic safety based on the driver's eye movement characteristics.

2.2. Driving Safety of the Tunnel Based on the Driver's Visual Load. Considering drivers are responsible for over 90% of road traffic crashes [8], it is necessary to study the effects of driver behaviors on road safety. Based on the cognitive load theory [9], the road signs would increase the number and length of off-road glances, thereby creating external disturbances and hindering driver performance [10]. Unlike the billboard on which information was not deeply processed by the driver, traffic signs required the driver's more cognitive load and caused greater distraction [11]. When the road environment was complicated, the driver's cognitive load has a significant impact on road safety [12].

Visual load is an important component of cognitive load. Since the magnitude of the visual load was closely related to the level of driving safety, appropriate reduction of the visual load was a necessary guarantee for driving safety [13, 14] and the eye movement is widely used to analyze the magnitude of visual load [15–17]. By counting the fixation duration and the number of saccades, the eye movement and brain waves were used to compare the effect of multi- and single-board directional road signs on expressways safety, and the result showed that the multi-board signs are more risky [18]. In terms of influencing factors, the visual load had a strong correlation with pupil, blink rate, saccade range, fixation duration, and field size [19, 20].

The relevant literature concerning drivers' visual load and tunnel driving safety shows that the visual load of drivers varies greatly in different areas of tunnel entrances and exits and under different weather conditions including daytime, dusk, and night [21, 22]. Meng introduced a new concept of exposure to traffic conflicts in urban road tunnel as the mean sojourn time in a given period that vehicles are exposed to dangerous scenarios and established a negative binomial regression model to reflect the relationship between the proposed exposure to traffic conflicts and crash

count [23]. Kinateder studied the influence of information with or without additional virtual reality behavior training on self-evacuation in the case of a simulated highway tunnel emergency [24]. At entrances and exits of the highway tunnel, visual oscillation was introduced to analyze the phenomenon of driver's transient blind period [13]. Winsum found that the visual tunnel effect would increase by the task time in the process of driving [25]. For very long road tunnels, Mehri investigated the disability glare problem and proposed the improvement path of the tunnel lighting system from visibility level, overall uniformity, and longitudinal uniformity perspectives [26].

For tunnels in high-altitude areas, there were special environmental and tunnel design parameters different from tunnels in plain areas. Comparing drivers' eye movement characteristics and psycho-physiological reactions at tunnel entrances in plain and high-altitude areas respectively, Yan found that the pupil size is mainly related to the ambient illuminance and showed a greater change of rate in pupil diameter in illuminance at tunnel entrances to fewer lights in high-altitude areas [27]. Shang compared the drivers' eye gaze behavior in the tunnel group with the single tunnel based on the Markov chain and, the result showed that the design and management of tunnel groups were more complex than that of a single tunnel. The longer the tunnel, the greater the difference [28, 29].

Existing literature mainly focuses on the impact of driver's bad driving behavior on driving risks and the analysis of traffic safety in urban tunnels. However, there are few studies about long tunnels in mountain highways, and studies on the evaluation of tunnel driving risks from the perspective of eye movement load are extremely rare. In fact, tunnels in the mountain highways have serious traffic safety risks. It is necessary to study the physiological and psychological changes of drivers in long tunnels and their influence on traffic safety based on eye movement characteristics.

2.3. Application of the Support Vector Machine Model in Transportation Field. Support Vector Machine (SVM) classification models are often used in traffic monitoring. Based on the global positioning system, SVM was used to identify stop and forward behavior of vehicle trajectory [30]. According to the city's road network adequacy, traffic flow, speed, and occupancy data, SVM was used to identify five types of urban traffic states, which included smooth, basically smooth, slight congestion, moderate congestion, and severe congestion [31]. Based on the cellular event data, the candidate feature set could be extracted by cell switching and position updating. Then the feature set was corresponding to the traffic state, position, and time interval, and the SVM classifier could be used to detect the traffic state of the main road [32]. Through the image data collected by UAV at urban intersections, the SVM classifier could extract vehicle type, position, speed, and trajectory characteristics, thus realizing the detection of safe space between vehicles [33].

Support Vector Regression (SVR) is often used in traffic flow prediction and traffic safety analysis. Based on the real-time detection data of Yan'an highway in Shanghai, China, SVR can be combined with wavelet analysis to build a short-term traffic speed prediction mode, which can be used to explore the relationship between traffic flow, traffic speed, and average occupancy rate [34]. Based on the data of flow, speed, the standard deviation of speed, density, density change, and proportion of vehicles of each type, SVR could be combined with logistic regression to establish a highway accident detection model [35]. According to the time variation characteristics of physiological signal, driver control input, vehicle kinematics, and weather, SVR can be combined with Bayesian learning to predict traffic collision accidents in real time [36].

In recent years, literature have begun to discuss traffic safety issues from the perspective of driver behavior. Chai selected steering wheel steering ratio, the proportion of steering wheel stationary time, times of steering wheel maintaining stability, and the percentage of steering wheel angular speed to represent driver status and used the driving simulator to collect data and establish a multi-level ordered evaluation model based on Support Vector Machine [37]. Rahman discussed the safety behavior of drivers at signalized intersections [38]. According to the collected vehicle attribute data such as speed, position, and arrival time, combined linear support vector machine, polynomial support vector machine, and artificial neural network are used to predict driver behavior under the dilemma of the time change and speed change, thereby improving signal operation at intersections. However, the analysis of driver behavior in mountain tunnels in the existing literature is rare.

In summary, scholars focus on the characteristics of drivers' visual load and traffic safety in tunnels, but few literature have analyzed the traffic safety in tunnels from the perspective of visual load, and traffic safety in mountain highway tunnels was ignored. Therefore, this paper takes the Gaogu length tunnel in the mountain highway as the research object, the driver's pupil area change rate as the research parameter, and the maximum instantaneous speed value of the pupil area and the duration of visual shock as the evaluation index to quantitatively study the visual load. Then the GA-SVR model of MTPA influencing factor evaluation was constructed to analyze the influences of speed, design brightness, measured brightness, and position in five stages to find out ways to improve driving safety in the long tunnel of mountain highway.

3. Methods

3.1. Test Tunnel and Drivers. Gaogu Long Tunnel on the mountainous highway was selected as the actual vehicle test section where the total length was 1,270 m. The appearance of Gaogu Long Tunnel seen from the car is shown in Figure 1. The speed limit of the tunnel was 80 km/h, which was one-way and two-lane with double holes, and an average

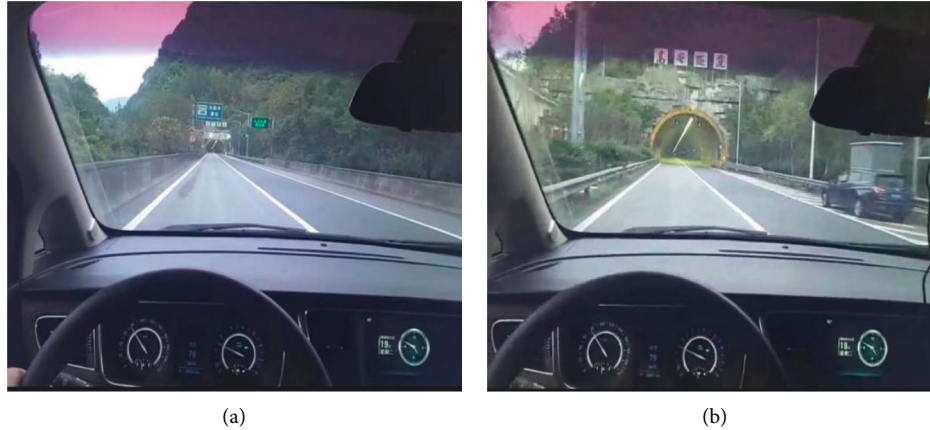


FIGURE 1: Gaogu Long Tunnel.

longitudinal slope of less than 2%. Seven males aged between 25 and 56 years were selected as test drivers. They have corrected visual acuity above 5.0 and C1 driving license. They got enough sleep the night before the test, avoided strenuous exercise, and avoided smoking and drinking alcohol, tea, coffee, and drugs that may affect the test results.

3.2. Test Equipment. A seven-seater commercial vehicle was selected as the test vehicle. In the experiment, the eye-tracking data acquisition equipment was the SMI2.1 spectacle-type eye tracker from SMI, Germany. The eye tracker had a sampling frequency of 60 Hz and a tracking accuracy of 0.1° . The speed of the vehicle was collected by a non-contact multifunctional speed meter and the measurement range was 0–300 km/h. The measured brightness data acquisition equipment LX-9621 illuminance meter, the measurement range was 0–50000 Lux. The device of the experiment is shown in Figure 2.

3.3. Experimental Procedures and Data Collection. To reduce the interference of traffic volume on the test, the test time was from 10:00 to 16:00 from Tuesday to Thursday when the traffic volume was less, and the test was carried out when the weather was fine. The drivers were informed to drive according to their driving habits and pay attention to driving safety before the test. The collected pupil data was extracted using BeGaze3.5 data analysis software.

3.4. Characterization of MTPA Visual Load. The change in pupil area is an ideal indicator to measure the psychological and physiological load of the driver. The larger pupil area often means a larger eye movement load. The pupil area of the driver changes rapidly with the sudden change of the light environment at the entrance and exit of the tunnel in a short period of time. The weighted acceleration root mean square can be used to evaluate the instantaneous vibration of the human body [39], then, the continuous weighted speed average of the pupil area root value can be used to evaluate the size of visual load:

$$Ve_k(t_0) = \left[\frac{1}{f} \int_{t_0}^{t_0} V_w^2 dt \right]^{1/2}. \quad (1)$$

In formula (1), $Ve_k(t)$ is the pupil area change speed, f is the continuous average integration time, integral variable t is the time, t_0 is the instantaneous investigation time, and V_w is the pupil area change speed.

Considering the discrete time points of the pupil diameter index collected in the driving visual load test in seconds, the maximum transient speed value of pupil area can be defined as

$$Ve_{MTPA} = \max\{Ve_k(t_0)\}. \quad (2)$$

The unit of MTPA is mm^2/s . When measuring the MTPA in the entrance and exit of the tunnel, f is usually equal to 1 s.

3.5. GA-SVR Model. Compared with the traditional linear regression model, the support vector regression (SVR) can in the case of a small sample and nonlinear data get the global optimal solution, so that in the short term MTPA prediction can maximize the mining position, speed, design brightness, measured brightness the implied information in the experimental data. In the process of prediction, SVR depends greatly on the penalty parameters and kernel function of variance, but the setting of these two parameters is often subjective or based on the past experience. Genetic algorithm (GA) has the advantages of group search and inherent heuristic random search, and it is not easy to fall into the local optimum. In view of this, this paper combines a genetic algorithm and support vector regression algorithm and uses the advantages of GA to obtain the key parameters in the SVR model, and then obtains more accurate short-term MTPA prediction results.

3.5.1. Support Vector Regression (SVR). The basic idea of SVR is to map the value to the high-dimensional feature space through a nonlinear mapping function and perform linear regression in this space to form the optimal decision function. $\{(x_i, y_i), i = 1, 2, \dots, m\}$ is marked as the training

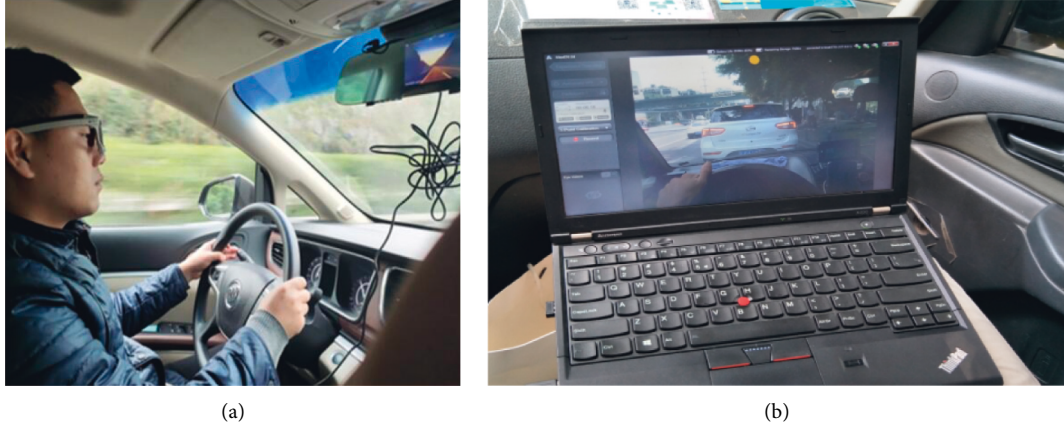


FIGURE 2: Device of experiment.

set containing m training samples, in which $x_i = [x_i^1, x_i^2, x_i^3, x_i^4]^T$ represents the input column vector of the sample i and $y_i \in R$ represents the corresponding MTPA observation value. In particular, x_i^1 represents the speed, x_i^2 represents the design brightness, x_i^3 represents the measured brightness, and x_i^4 represents the position. The optimal decision function $f(x)$ is defined as follows:

$$f(x) = \omega\varphi(x) + b. \quad (3)$$

In formula (3), ω is the weight vector, $\varphi(x)$ is the nonlinear mapping function, and b is the threshold. Further,

the insensitive loss function ε was introduced to obtain the loss function:

$$L(x_i, y_i, f_i) = \max\{|y_i - f(x_i)| - \varepsilon, 0\}. \quad (4)$$

According to formula (4), if the difference between the observed value y_i of x_i and the predicted value $f(x_i)$ is less than ε , the loss value is 0. When the condition of ε is satisfied, ω must be minimized, that is $\min 1/2\|\omega\|$. To solve the problem that ε cannot be estimated, slack variables ξ_i and ξ_i^* are introduced, and SVR is transformed into the following minimization problem.

$$\min \frac{1}{2}\|\omega\|^2 + C \sum_{i=1}^m (\xi_i + \xi_i^*) \text{ s.t. } \begin{cases} y_i - \omega\varphi(x) - b \leq \varepsilon + \xi_i \\ \omega\varphi(x) + b - y_i \leq \varepsilon + \xi_i^* \\ \xi_i \geq 0 \\ \xi_i^* \geq 0 \end{cases} \quad i = 1, 2, 3, \dots, m. \quad (5)$$

In formula (5), the penalty parameter is denoted as C . The larger the C , the greater the penalty for the samples with

training errors greater than ε . Using duality principle to transform equation (5) as follows:

$$\max_{a, a^*} \left[-\frac{1}{2} \sum_{i=1}^m \sum_{j=1}^m (a_i - a_i^*)(a_j - a_j^*) K(x_i, x_j) - \sum_{i=1}^m (a_i - a_i^*)\varepsilon + \sum_{i=1}^m (a_i + a_i^*)y_i \right]. \quad (6)$$

In formula (6), $K(x_i, x_j)$ is the radial basis kernel function:

$$K(x_i, x_j) = \exp\left(-\frac{\|x_i - x_j\|^2}{2\sigma^2}\right). \quad (7)$$

In formula (7), σ^2 is the kernel function parameter.

The MTPA value in the experiment is denoted as $a = [a_1, a_2, a_3, \dots, a_m]$, and the optimal predicted value is $a^* = [a_1^*, a_2^*, a_3^*, \dots, a_m^*]$. Then the optimal linear regression function's coefficient ω^* and constant term b^* can be find as follows, in which N_{nsv} is the number of Support Vectors whose parameters the parameters of $(a_i - a_i^*)$ are not zero.

$$\omega^* = \sum_{i=1}^m (a_i - a_i^*) \varphi(x_i),$$

$$b^* = \frac{1}{N_{\text{nsv}}} \left\{ \sum_{0 < a_i < C} \left[y_i - \sum_{x_j \in \text{SV}} (a_i - a_i^*) K(x_i, x_j) - \varepsilon \right] + \sum_{0 < a_i < C} \left[y_i - \sum_{x_j \in \text{SV}} (a_j - a_j^*) K(x_i, x_j) + \varepsilon \right] \right\}. \quad (8)$$

3.5.2. *Genetic Algorithm in SVR.* As a popular evolutionary algorithm, its basic principle is to imitate the evolutionary law of “natural selection by nature and survival of the fittest.” In the process of optimizing the parameters of the SVR model, the genetic algorithm (GA) encodes the parameters into chromosomes and then exchanges the chromosome information in the population in an iterative manner, and finally generates chromosomes that meet the optimization goals. The parameter optimization process is shown in Figure 3:

According to Figure 3, the optimization process mainly includes the following steps:

Step 1: *Population Initialization.* The penalty parameters C and kernel function of variance parameters σ^2 in the SVR model were encoded.

Step 2: calculate the fitness value. The fitness value is used to evaluate the pros and cons of individuals in the population to facilitate the selection of individuals. The absolute value of the deviation between the error prediction value $F(x_i)$ and the actual error value Y_i is used as the fitness value H . The fitness function as follows:

$$H = g \left(\sum_{i=1}^m \text{abs}(F(x_i) - Y_i) \right). \quad (9)$$

Step 3: *Selection Operation.* The individual i was randomly selected from the original population by roulette method for population recombination operation. The probability of individual selection was as follows:

$$P_i = \frac{H_i}{\sum_{i=1}^m H_i}. \quad (10)$$

Step 4: *Crossover Operation.* Select two individuals from the original population and perform crossover recombination operations. The new generation of individuals contains the excellent characteristics of the previous generation. Marked λ as the random number in $[0, 1]$, the intersection of chromosomes β_k and β_h at the position i was as follows:

$$\begin{aligned} \beta_{ki} &= \beta_{ki}(1 - \lambda) + \beta_{hi}\lambda, \\ \beta_{hi} &= \beta_{hi}(1 - \lambda) + \beta_{ki}\lambda. \end{aligned} \quad (11)$$

Step 5: *Mutation Operation.* To avoid obtaining the local optimal solution, individuals carry out random variations to seek population diversity. β_{il} represented the mutation of the l -th gene of the i -th individual:

$$\beta_{il} = \begin{cases} \beta_{il} + (\beta_{il} - \beta_{\max}) * \theta \left(1 - \frac{k}{G_{\max}} \right)^2, & r > 0.5, \\ \beta_{il} + (\beta_{\min} - \beta_{il}) * \theta \left(1 - \frac{k}{G_{\max}} \right)^2, & r \leq 0.5. \end{cases} \quad (12)$$

In formula (12), β_{\min} and β_{\max} are the upper and lower limits of the selected gene, k is the current number of iterations, r and θ were random number between $[0, 1]$; G_{\max} is the maximum iteration number. When the number of algorithm iterations reaches the maximum, the penalty parameters C and kernel function of variance parameters σ^2 in the SVR model complete the optimization.

4. Results

4.1. *Experimental Data Description and Stage Division.* Taking the entrance of the long tunnel as the origin, data of the driver's pupil, vehicle position, driving speed, design brightness inside and outside the tunnel, and the measured brightness of the experimental vehicle in the process of entering and leaving the tunnel were collected. After removing abnormal data, 2,625 experimental data were obtained. The experimental data of seven people were averaged, and a total of 375 samples were obtained. The relationship between speed, design brightness, measured brightness, MTPA, and position is shown in Figure 4.

As can be seen from Figure 4, speed, design brightness, and measured brightness all have significant stage characteristics. In terms of speed, when driving close to the tunnel entrance section where the position was from -300 m to 0 m, the speed decreased from 100 km/h to 80 km/h. When driving in the tunnel where the position was from 0 m to 1270 m, the speed was maintained between 70 and 80 km/h. After exiting the tunnel, the speed quickly increased to 110 km/h. The periodic variation of speed can be attributed to the speed regulation of mountain highway tunnel. According to China's "Road Traffic Safety Law," the speed in mountain highway tunnels should be below the speed limit of 80 km/h; in addition, design brightness and measured brightness decreased from $4,500$ cd/m² before entering the tunnel to 10 cd/m² in the tunnel, then increased to $4,500$ cd/m² after exiting the tunnel.

According the relationship between MTPA and position in Figure 4(d), at the beginning of the experiment, MTPA was below 10 mm²/s and the driver felt comfortable; from 200 m before the tunnel, MTPA began to increase rapidly until 45 mm²/s at 50 m after the entrance, and then gradually fall back; after entering the tunnel 200 m, the driver began to adapt to the tunnel environment and the MTPA value

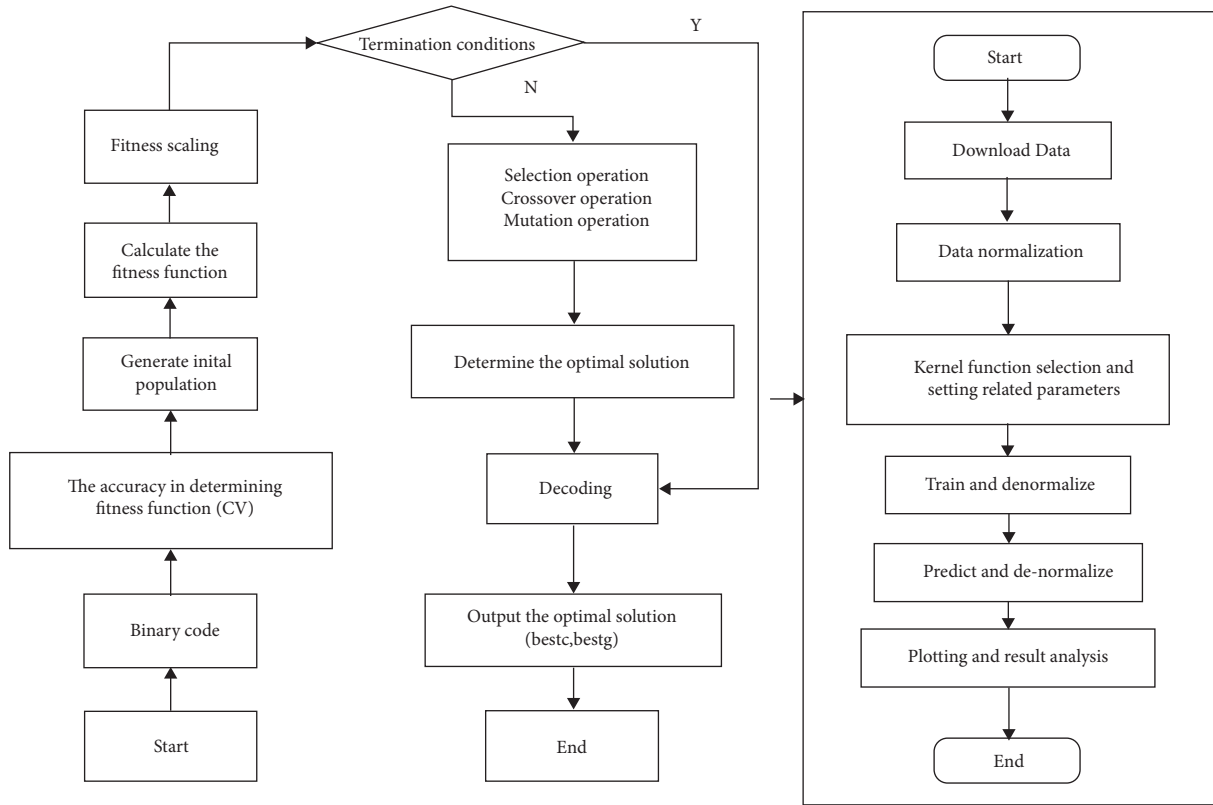


FIGURE 3: GA-SVR algorithm flow chart.

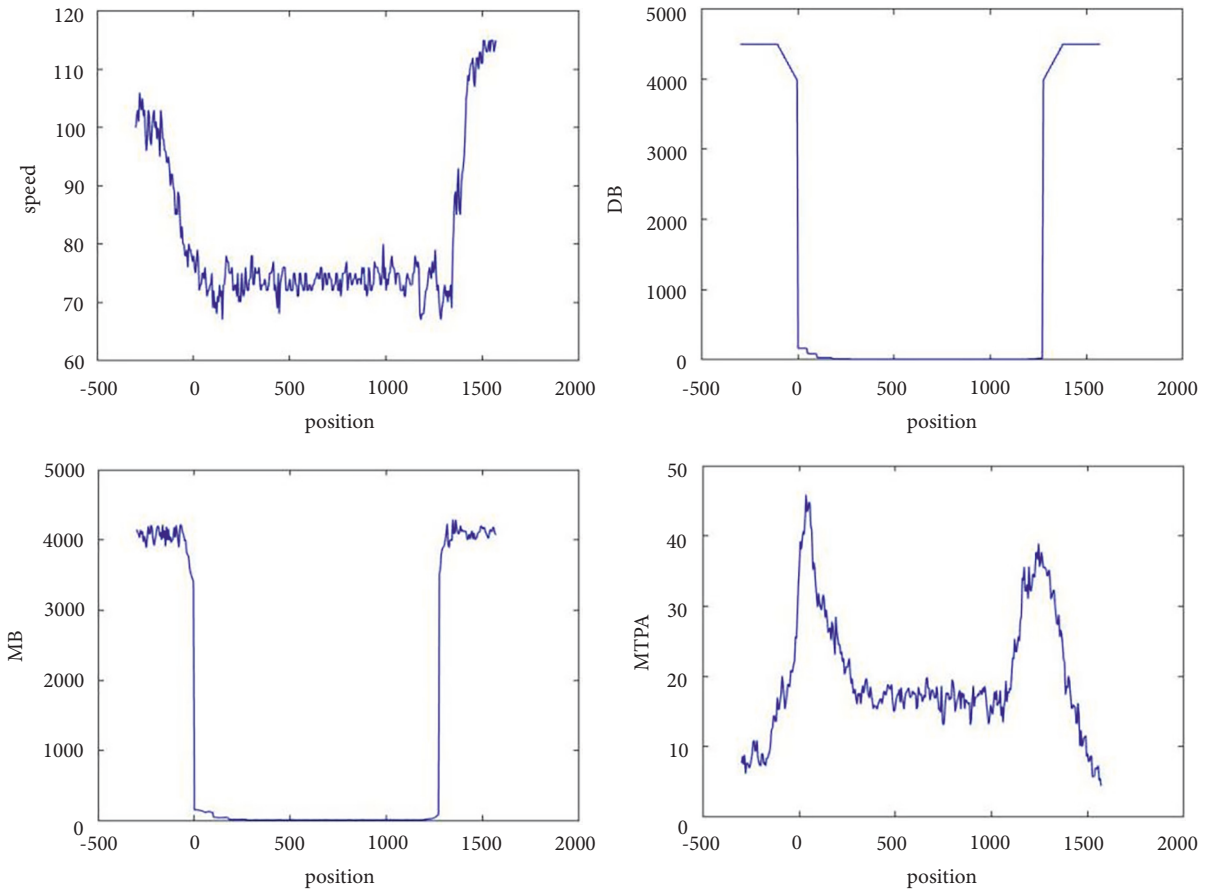


FIGURE 4: The relationship between speed, design brightness, measured brightness, MTPA, and position.

fluctuated steadily in the range of 10–20 mm²/s; after the exit of the tunnel was visible to the driver, MTPA increased rapidly again more than 30 mm²/s and peaked at 39 mm²/s in the 30 m after the exit. Therefore, the driver's position perception has a significant impact on MTPA changes.

In previous studies, the research objects were mostly the short tunnels on urban roads, then the research stage is usually divided into three parts, which included entrance, inside the tunnel, and exit. But it is rare to take long tunnels on mountain highways as the research object. In addition, the existing research mainly studied the influence of single or double factors on drivers' eye movement state [40], but rarely comprehensively analyzed the influence of four factors including position, speed, design brightness, and measured brightness. The influence of factors on the driver's psychology. However, the experimental data showed that the MTPA should be divided into five stages in the long tunnels of mountain highways, including steep increasing, falling steady, fluctuation, sharp increasing again, and falling again. Therefore, this paper divides the position range into five sections to discuss the influencing factors of MTPA, namely (−300 m, 0), (0, 200 m), (200 m, 1070 m), (1070 m, 1270 m), and (1270 m, 1570 m).

4.2. GA-SVR Model. In this paper, a GA-SVR model for calculating MTPA is established by taking speed, design brightness, measured brightness, and position as input variables and MTPA value as the output variable.

In the process of obtaining the penalty parameters and kernel function of variance parameters in SVR model by genetic algorithm, evolution times were set to 200, population size was set to 20, crossover probability parameter was set to 0.7, mutation probability parameter was set to 0.035, and the optimization range was set to [0, 100]. To minimize the mean square error (MSE), the fitness function was established to search for the optimal penalty parameters C and kernel function's variance parameters σ^2 in the SVR model, and the result is shown in Figure 5.

It can be seen from Figure 5 that MSE achieves convergence after 15 evolutions, and the minimum value is 0.012. At that time, the corresponding penalty parameters C and kernel function's variance parameters σ^2 are equal to 17.5126 and 13.712, respectively. Further, 281 samples were randomly selected from 375 valid samples as the training set and the remaining 94 samples as the test set. After putting the optimal parameters into the SVR model and calling the Libsvm toolbox in MATLAB, the optimal model can be obtained after 300 iterations and the prediction effect is shown in Figure 6. The results showed that the mean square error between the predicted and the actual value is 0.0064813, and the determination coefficient was 0.96384. In other words, the four factors including speed, design brightness, measured brightness, and position can explain 96.38% variation of MTPA.

4.3. Analysis of Influencing Factors of MTPA Based on the GA-SVR Model. The influence of speed, design brightness, measured brightness, and position on MTPA were

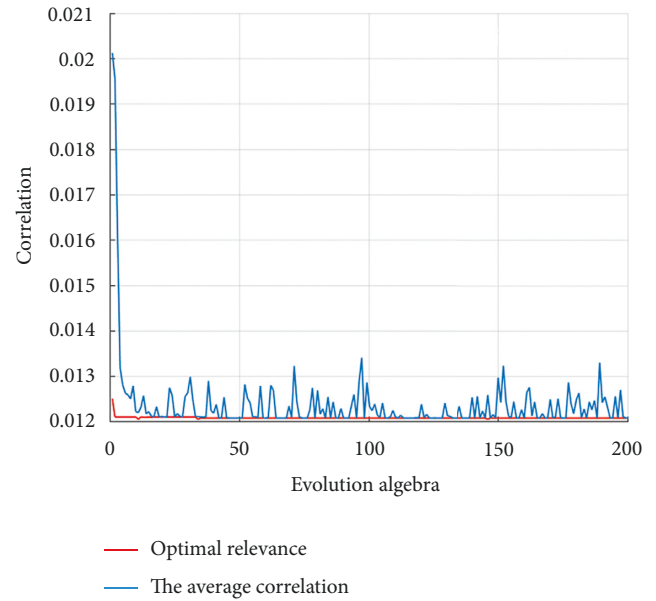


FIGURE 5: Optimal parameters.

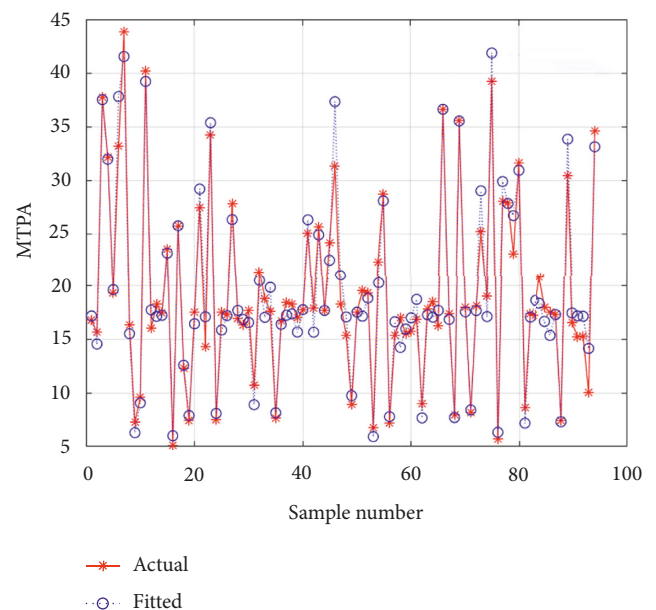


FIGURE 6: SVR model prediction results.

compared by analyzing the sensitivity of GA-SVR model, and the sensitivity analysis results are shown in Table 1.

Comparing the rows in Table 1 shows that the main factors affecting MTPA are not the same in each stage: in stage 1, the sensitivity of MTPA to position and speed is higher, 17.31% and 12.08% respectively; in stage 2, MTPA is relatively sensitive to changes in position and speed, with sensitivities of 2.96% and 2.92% respectively; in stage 3, MTPA is relatively sensitive to changes in design brightness, with a sensitivity of 1.42%; in stage 4, the sensitivity of MTPA to position and speed is higher, 36.27% and 7.21% respectively; in stage 5, the sensitivity of MTPA to position and the design brightness is higher, 47.71% and 12.87%

TABLE 1: The sensitivity analysis of MTPA.

Stage	Interval	Speed (%)	Design brightness (%)	Measured brightness (%)	Position (%)
1	(-300, 0)	12.08	4.0	1.85	17.31
2	(0, 200]	2.92	<0.01	0.01	2.96
3	(200, 1070]	0.20	1.42	0.11	0.80
4	(1070, 1270]	7.21	<0.01	<0.01	36.27
5	(1270, 1570]	1.50	12.87	5.12	47.71

respectively. In addition, the sensitivity of MTPA varies with stages, and the sensitivity of MTPA in stage 1, 4, and 5 is relatively high.

Comparing the columns of Table 1, it can be found that the sensitivity of each influencing factor at different stages is not the same: the speed sensitivity is higher in stage 1 and stage 4, 12.08% and 7.21% respectively; the design brightness sensitivity is higher in stage 1 and stage 5, 4.0% and 12.87% respectively; the measured brightness sensitivity is higher in stage 1 and stage 5, 1.85% and 5.12% respectively; the position sensitivity is higher in stage 1, stage 4, and stage 5 is, respectively 17.31%, 36.27%, and 47.71%.

Therefore, the following conclusions can be drawn from Table 1: First, the sensitivity of the designed brightness and the measured brightness at the entrance and exit of the tunnel is relatively high, which is consistent with existing studies [41]. Second, the speed is highly sensitive before entering and exiting the tunnel, which can be attributed to the speed monitoring method of the highway tunnel. In fact, the mountain highway tunnel adopts the speed monitoring method of interval speed measurement and the speed limit of 60–80 km/h is mandatory by law. Therefore, the driver will consciously control the driving speed before entering and exiting the tunnel. Last but not least, position is a major factor in MTPA during the three stages before entering the tunnel, before exiting the tunnel, and after exiting the tunnel. This can be explained by the complex terrain conditions and changeable climate conditions of the long tunnel in the mountain highway, so the abrupt change of the tunnel entrance section has a great influence.

5. Discussion

Unlike MPTA in urban tunnels, which is mainly affected by design brightness and measured brightness, the position is a key factor affecting MTPA in mountain highway tunnels, which are long in length and located in more complex terrain conditions. Therefore, it is necessary to combine position factors to further explore the influence of speed, design brightness, and measured brightness on MTPA at different stages.

5.1. The Effect of Speed and Position on MTPA. In this experiment, the speed range of stage 1 is 76–106 km/h, stage 2, stage 3, and stage 4 speed range is 65 km/h–80 km/h, and stage 5 speed range is 67 km/h–115 km/h. The average of the design brightness and the measured brightness and the GA-SVR model are used to simulate the influence of the speed and position on the MPTA.

Figure 7 shows the impact of speed and position on MTPA when a vehicle enters a long tunnel. It can be seen that the range of MTPA value is (5, 17) in stage 1, and it abruptly increases to (25, 35) in stage 2, and is (15, 20) in stage 3. Comparing the height of the MTPA in the three sub-graphs, it can be found that when the vehicle enters the tunnel, the MTPA value experienced a significant increase from stage 1 to stage 2, and then decreased slightly from stage 2 to stage 3. This can be explained as the result of the combined effect of the speed control of the mountain highway and the black hole effect.

From Figure 7(a), it can be found that the driving speed in stage 1 is reduced from 110 km/h to 70 km/h, and the closer to the entrance, the higher the MTPA. This can be explained as the speed control mark and black hole effect will urge the driver to be more vigilant. From the Figure 7(b), MTPA in stage 2 is higher when the speed is closer to the speed limit of 80 km/h or closer to the hole. This can be explained by the rapid change of the driving environment at the moment of entering the tunnel, which causes the driver's stress to soar. After that, MTPA decreases as the driving environment in the tunnel adapts and the speed slows down. From the Figure 7(c), the fluctuation of the MTPA is small in stage 3. The closer the speed is to the limit of 80 km/h, the higher the MTPA value. As the tunnel deepens and the driver realizes the pressure brought by the long tunnel environment, the MTPA gradually decreases and stabilizes in the high-value range, which is still higher than stage 1.

Figure 8 shows the impact of vehicle speed and position on MTPA during the process of driving out of a long tunnel. It can be seen that the variation range of the MTPA value is (15–20) in stage 3, suddenly increases to (25–35) in stage 4, and decreases to (5–15) in stage 5. Comparing the height of the MTPA in the three sub-graphs, it can be found that the MTPA value has experienced a significant increase from stage 3 to stage 4, and then a drastic decrease from stage 4 to stage 5 when the vehicle leaves the long tunnel. This can be explained as the result of the combined effect of speed control and the white hole effect on mountain highways.

Figure 8(b) shows the MTPA suddenly increased after the driver saw the exit in stage 4. Speed and position have a synergistic effect on MTPA. The closer the speed is to 80 km/h or the position is to the exit, the higher the MTPA. It can be explained as the white hole effect and the driver's worry about unknown mountain terrain and climate conditions after driving out of the tunnel. Figure 8(c) shows the MTPA gradually decreased as the vehicle move further away from the exit in stage 5, even if the driving speed increases from 70 to 115 km/h. This can be explained as the psychological pressure of the driver was effectively released after driving

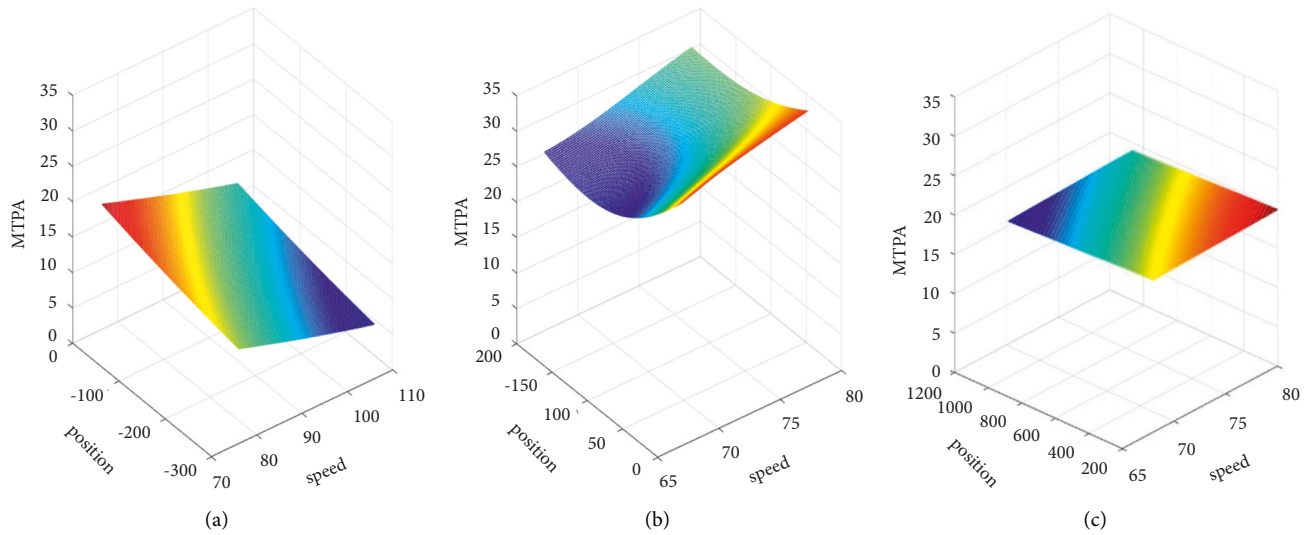


FIGURE 7: The influence of speed and position on MTPA in stages 1–3. (a) Stage 1. (b) Stage 2. (c) Stage 3.

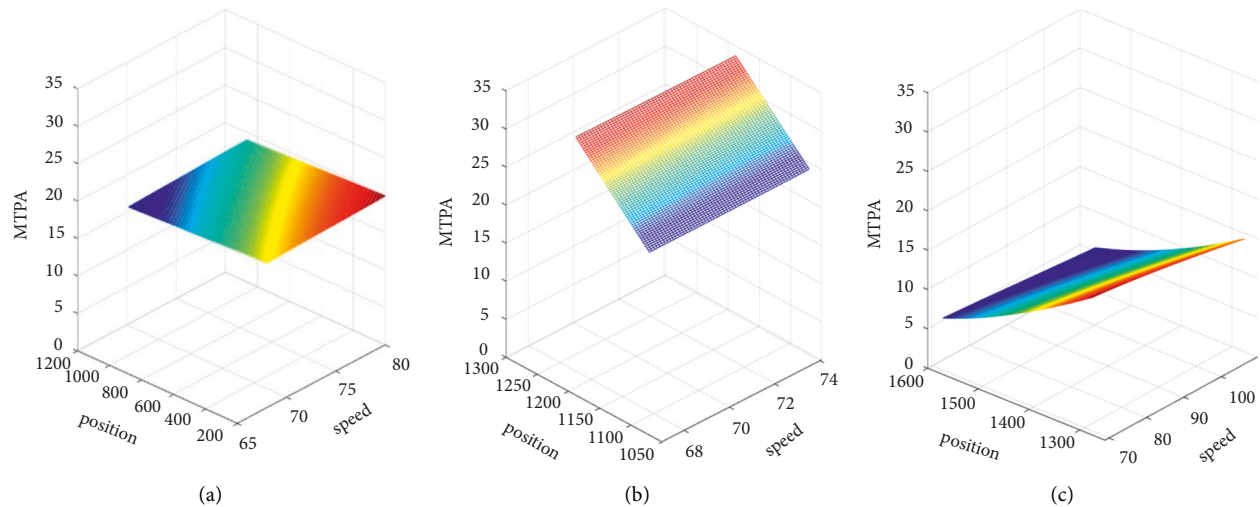


FIGURE 8: The influence of speed and position on MTPA in stages 3–5. (a) Stage 3. (b) Stage 4. (c) Stage 5.

out of the tunnel. It can be inferred that position has a greater effect on MTPA than speed.

Existing research shows that the speed should be proportional to MTPA in the ordinary tunnel [42]. However, this classical assumption is not valid in stage 1 and stage 5 of the long tunnel on the mountain highways because position has a greater effect on MTPA than speed in these two stages. Therefore, when setting the speed limit or warning signs for long tunnels of mountain highways, it is necessary to carefully consider the starting position of signs.

5.2. The Effect of Design Brightness and Position on MTPA.

For the long tunnel in the mountain highway, the design brightness in stage 1 is reduced from 4500 to 4000 cd/m^2 , further down from 160 to 8 cd/m^2 in the stage 2. In stage 3 where the tunnel was deep, the design brightness fluctuated between 3 and 8 cd/m^2 . In the stage 4, where the driver can

see the tunnel exit, the design brightness range is 3 ~ 15 cd/m^2 . After exiting the tunnel, the design brightness in stage 5 increases from 4000 cd/m^2 to 4500 cd/m^2 . Take the average speed and the measured brightness, and the GA-SVR model is used to simulate the influence of the design brightness and position on the MPTA.

Figure 9 shows the influence of the design brightness and position on the MTPA when the vehicle driving in the long tunnel. The range of MTPA value is (4, 13) in stage 1, then abruptly increases to (20, 40) in stage 2, and decreases to (18, 23) in stage 3. Comparing subgraphs, it can be found that when the vehicle enters the tunnel, the MTPA value has experienced a significant increase from stage 1 to stage 2, and then rapidly drops from stage 2 to stage 3 but remains high. The dramatic changes in MTPA can be explained by the black hole effect, which can be attributed to a sharp drop in the design brightness from 4000 cd/m^2 outside the tunnel to 160 cd/m^2 inside the tunnel. Although the MTPA of the

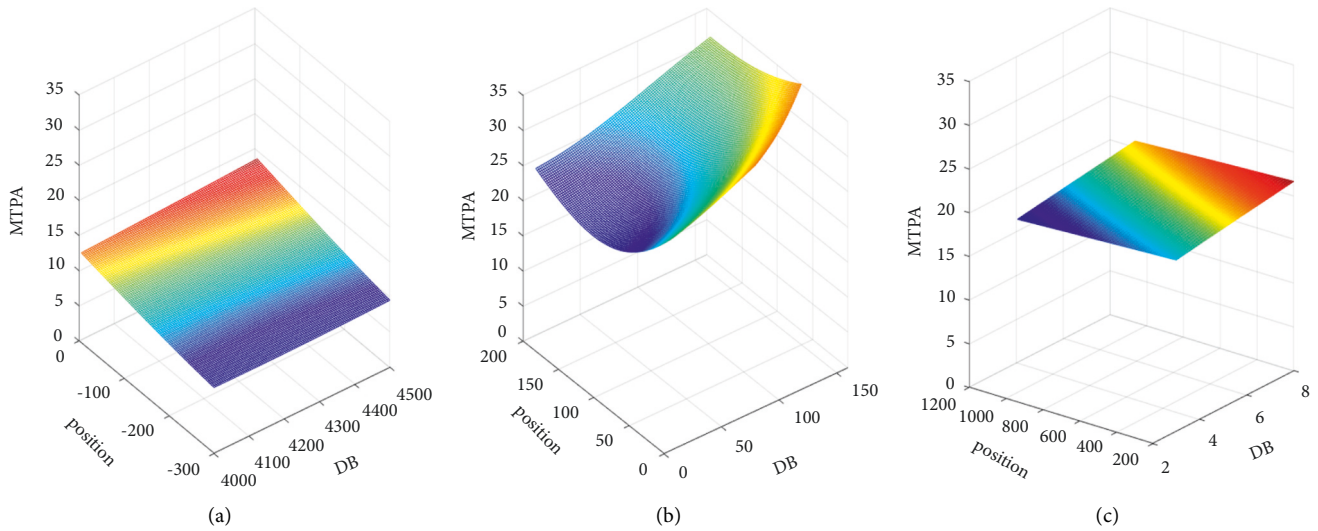


FIGURE 9: The influence of design brightness and position on MTPA in stages 1–3. (a) Stage 1. (b) Stage 2. (c) Stage 3.

third stage fell, it was still larger than that of the first stage. This phenomenon can be explained as the long-time closed driving environment brought by the long tunnel would increase the psychological load of drivers.

Figure 9(a) shows that MTPA is mainly affected by the position in stage 1. Figure 9(b) shows that MTPA reached the peak value at the moment when entering the tunnel, and then showed a trend of first decreasing and then increasing in stage 2. This phenomenon can be explained as the gradual lighting design of the entrance section can effectively alleviate the visual discomfort of the driver when entering the tunnel. Figure 9(c) shows that MTPA fluctuates steadily in stage 3 and is still directly proportional to the design brightness.

Figure 10 shows the influence of design brightness and position on MTPA in the process of the vehicle leaving a long tunnel. The range of the MTPA is (18, 23) in stage 3, suddenly increases to (20, 35) in stage 4, and decreases to (10, 15) in stage 5. Comparing three sub-graphs, it can be found that during the process of vehicles leaving the tunnel, the MTPA value has experienced a significant increase from stage 3 to stage 4, then a sharp drop from stage 4 to stage 5. It can be attributed to the stage jump of the design brightness from 15 cd/m^2 at the exit of the tunnel to 4000 cd/m^2 outside the tunnel.

Besides, Figure 10(b) shows that the effect of position on MTPA is greater than the design brightness in stage 4. Although the design brightness just increases from 3 to 15 cd/m^2 , the MTPA increases sharply at this time and reaches the peak when it approaches the tunnel entrance. Figure 10(c) shows that MTPA fluctuated steadily in stage 5. The design brightness and position have no significant influence on MTPA after exiting the tunnel.

The changes in MTPA indicate that the design brightness should be inversely proportional to the MTPA, which is consistent with existing research [43]. However, it is interesting that this conclusion is not true in stage 2 and stage 4 for the long tunnel of mountain highway. The reason is that

the design of the gradual lighting section in stage 2 can effectively alleviate the visual discomfort when the driver just enters the tunnel, and the influence of the position in stage 4 played a decisive role. Different from plain areas, mountain highways may face a more complex driving environment after exiting the long tunnel, such as re-entering the tunnel, more complex terrain structure, rainy and foggy climate, and so on. The unknown driving environment after the long tunnel leads to an increase of psychological pressure. Therefore, it is necessary to consider a more refined gradual lighting design in stage 2 and stage 4. Moreover, it is particularly important to consider the starting position and setting the length of the gradual lighting section in stage 4.

5.3. The Effect of Measured Brightness and Position on MTPA.

Different from other literature, the measured brightness is specially added as the influencing factor of MTPA in this paper. For the long tunnel of the mountain highway, the measured brightness in stage 1 decreased from 4152 to 3408 cd/m^2 , further down from 152 to 15 cd/m^2 in the stage 2. In the stage 3, where the tunnel is deep, the measured brightness fluctuated between 5 and 18 cd/m^2 . In stage 4, the range of the measured brightness is $6 \sim 87 \text{ cd/m}^2$. After exiting the tunnel, the measured brightness in stage 5 increases from 3522 cd/m^2 to 4298 cd/m^2 . Take the average of speed and the design brightness, and the GA-SVR model is used to simulate the influence of the measured brightness and position on the MTPA.

Figure 11 shows the influence of the measured brightness and position on the MTPA when the vehicle enters the long tunnel. The range of MTPA value is (10, 15) in stage 1, then abruptly increases to (20, 35) in stage 2, and decreases to (5, 15) in stage 3. Comparing subgraphs, it can be found that when the vehicle enters the tunnel, the MTPA value has experienced a significant increase from stage 1 to stage 2, and then a rapid decline from stage 2 to stage 3. This can be explained as the result of the combined effect of the light

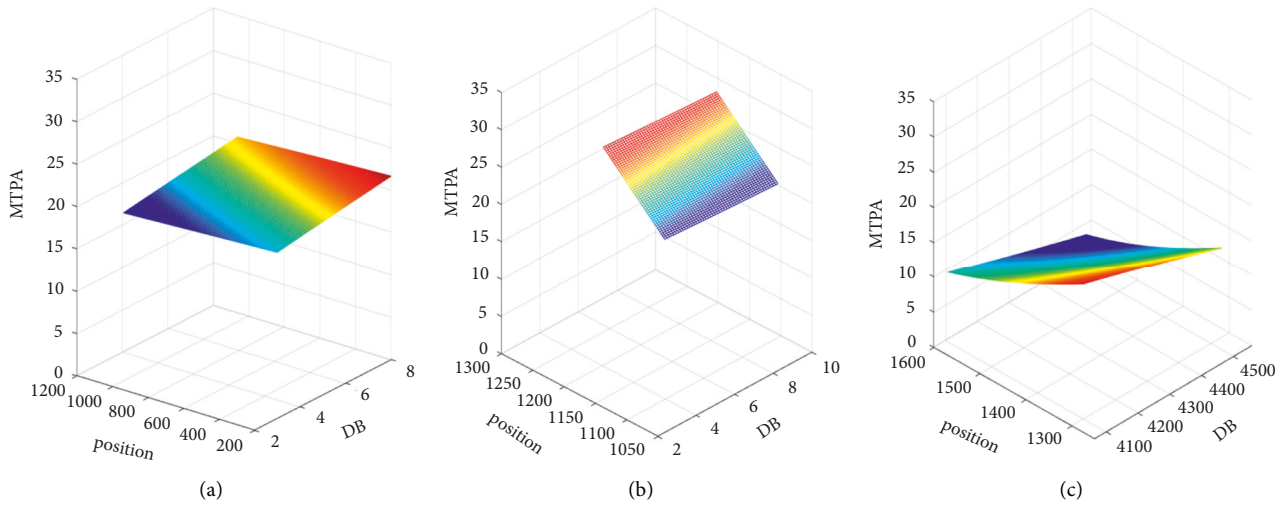


FIGURE 10: The influence of design brightness and position on MTPA in stages 3–5. (a) Stage 3. (b) Stage 4. (c) Stage 5.

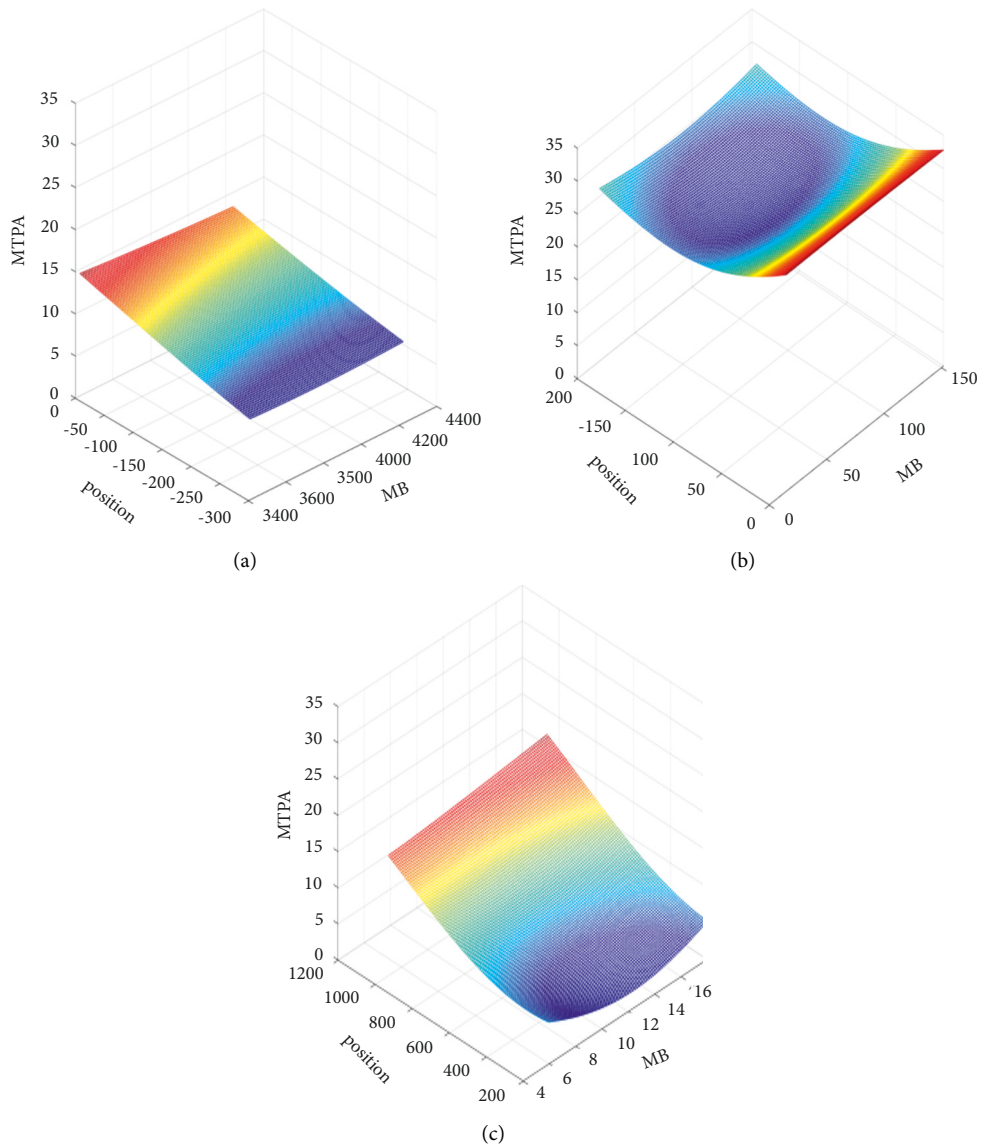


FIGURE 11: The effect of measured brightness and position on MTPA in stages 1–3. (a) Stage 1. (b) Stage 2. (c) Stage 3.

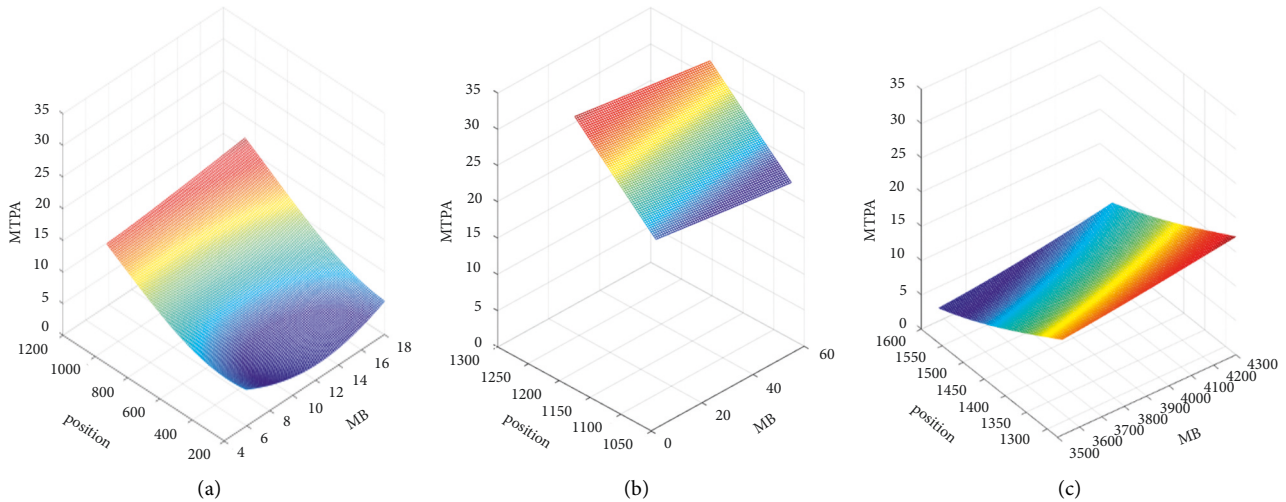


FIGURE 12: The effect of measured brightness and position on MTPA in stages 3–5. (a) Stage 3. (b) Stage 4. (c) Stage 5.

environment change and the position of the mountain highway.

Figure 11(a) shows that MTPA is mainly affected by the position in stage 1. The lower the measured brightness and the closer the vehicle is to the hole, the higher the driver's MTPA. Figure 11(b) shows that MTPA reached the peak value at the moment when entering the tunnel, then showed a trend of first decreasing and then stabilizing in stage 2. This phenomenon can be explained as the gradual lighting design of the entrance section can effectively enhance the ability to recognize the environment in the tunnel, so the driver can adapt to the black hole effect quickly. Figure 11(c) shows that the influence of position on MTPA is greater than that of measured brightness. As the vehicle deepens in the long tunnel, the MTPA shows a slow upward trend.

Figure 12 shows the influence of measured brightness and position on MTPA in the process of vehicle leaving a long tunnel. The range of the MTPA is (5, 15) in stage 3, suddenly increases to (20, 35) in stage 4, and decreases to (5, 15) in stage 5. Comparing three sub-graphs, it can be found that during the process of vehicles leaving the tunnel, the MTPA value has experienced a significant increase from stage 3 to stage 4, and then a sharp drop from stage 4 to stage 5. This can be explained as the influence of the white hole effect on the psychological changes of the driver.

Although the measured brightness just increases from 3 to 15 cd/m^2 , the MTPA increases sharply at this time and reaches the peak when it approaches the tunnel entrance. Figure 12(b) shows that MTPA fluctuated steadily in stage 5. The measured brightness and position have no significant influence on MTPA after exiting the tunnel.

Besides, Figure 12(b) shows that the effect of position on MTPA is greater than the measured brightness in stage 4. After the driver saw the tunnel exit, the MTPA increased sharply. The closer to the hole, the lower the measured brightness, the greater the MTPA. The MTPA is inversely proportional to the measured brightness change, which is consistent with the traditional view [44]. Figure 12(c) shows that the MTPA drops gradually as it moves away from the

tunnel, which means the psychological pressure of the driver is effectively released after exiting the tunnel.

6. Conclusions

With the development of mountainous highways in China in the past 10 years, the traffic safety risks in long mountainous highway tunnels have become a new issue. From the perspective of the drivers' visual load, this paper constructed a GA-SVR model of the influence of speed, design brightness, measured brightness, and the position on MTPA, and discussed the factors affecting driving safety in tunnels on mountain highways.

The conclusions showed that: firstly, the changes of MTPA in the long mountainous highway tunnels can be divided into five stages, which is different from the three-stage division of urban tunnels. This stage change is the result of the combined effects of speed, design brightness, measured brightness, and position; secondly, the influence degree of influencing factors is varied in different stages: the position factor matters most in stages 1, 2, 4, and 5. In stage 3, the design brightness has the greatest impact; thirdly, the comparison of stages indicated that stage 2 and stage 4 had the highest MTPA value, which suggested the greatest the driver's psychological pressure on the entrance and exit sections of the tunnel. This phenomenon explained the driver experienced the creation and disappearance of the "black hole effect" in stage 2, and the "white hole effect" and drastic changes in visual load in stage 4. This was consistent with the reality that the portals of the long tunnel were locations highly prone to traffic accidents. Therefore, it was necessary to consider a more accurate gradual lighting design in stage 2 and stage 4 and to consider the starting position and setting length of the gradual lighting section in stage 4; lastly, the MTPA value of stage 3 was significantly higher than that of stage 1 and stage 5 outside the tunnel. This showed that with the increased length of mountainous highway tunnels, the long-term enclosed driving environment made the psychological load of drivers intensify.

Therefore, it was necessary to enhance traffic safety management and protections in the middle of the tunnel.

The merit of this paper is the study on the influences of speed, design brightness, measured brightness, and position on the driver's eye movement. These factors can reflect the light setting and visual range characteristics of the long mountainous highway tunnels. In addition, SVR can analyze the nonlinear relationship between speed, design brightness, measured brightness, position, and MTPA with limited experimental data. Compared with the traditional cross search method, GA can optimize the parameters of the SVR, thereby increasing the accuracy rate from 89% to 96%. Therefore, GA-SVR is suitable for the safety risk assessment of the long mountainous highway tunnels [45–47].

Data Availability

The data are available upon request to the corresponding author.

Conflicts of Interest

The authors declare that they have no conflicts of interest.

Acknowledgments

This work was supported by the National Natural Science Foundation of China (No. 71901043), the Chongqing Municipal Education Commission Project (Nos. KJQN201900739 and KJQN201900722), and the Science and Technology Bureau Foundation and Frontier Project of Chongqing (Nos. cstc2019jcyj-msxmX0629 and cstc2019jcyj-msxmX0695).

References

- [1] China's Ministry of Transport, "Statistical Bulletin on the Development of the Transport Industry," *China's Ministry of Transport, China*, 2021, https://xxgk.mot.gov.cn/2020/jigou/zhghs/202205/t20220524_3656659.html.
- [2] H. S. Luo, Z. G. Du, and H. Zeng, "Study on the safety improvement effect of urban long tunnel guidance visual reference system," *Chinese Safety Science Journal*, vol. 30, pp. 154–159, 2020.
- [3] G. Vashitz, D. Shinar, and Y. Blum, "In-vehicle information systems to improve traffic safety in road tunnels," *Transportation Research Part F: Traffic Psychology and Behaviour*, vol. 11, no. 1, pp. 61–74, 2008.
- [4] Y. Wu, "Assessment of the impact of jet flame hazard from hydrogen cars in road tunnels," *Transportation Research Part C: Emerging Technologies*, vol. 16, no. 2, pp. 246–254, 2008.
- [5] M. M. Chatzimichailidou and I. M. Dokas, "RiskSOAP: introducing and applying a methodology of risk self-awareness in road tunnel safety," *Accident Analysis & Prevention*, vol. 90, pp. 118–127, 2016.
- [6] Q. Z. Hou, A. P. Tarko, and X. H. Meng, "Analyzing crash frequency in freeway tunnels: a correlated random parameters approach," *Accident Analysis & Prevention*, vol. 111, pp. 94–100, 2018.
- [7] X. H. Zhao, C. F. Zhang, Y. J. Ju, J. Li, Y. Bian, and J. M. Ma, "Evaluation of tunnel retro-reflective arch in an extra-long tunnel based on the matter-element extension method," *Accident Analysis & Prevention*, vol. 150, Article ID 105913, 2021.
- [8] E. K. Adanu, R. Smith, L. Powell, and S. Jones, "Multilevel analysis of the role of human factors in regional disparities in crash outcomes," *Accident Analysis & Prevention*, vol. 109, pp. 10–17, 2017.
- [9] P. Chandler and J. Sweller, "Cognitive load theory and the format of instruction," *Cognition and Instruction*, vol. 8, no. 4, pp. 293–332, 1991.
- [10] D. B. Kaber, Y. Liang, Y. Zhang, M. L. Rogers, and S. Gangakhedkar, "Driver performance effects of simultaneous visual and cognitive distraction and adaptation behavior," *Transportation Research Part F: Traffic Psychology and Behaviour*, vol. 15, no. 5, pp. 491–501, 2012.
- [11] T. Dukic, C. Ahlstrom, C. Patten, C. Kettwich, and K. Kircher, "Effects of electronic billboards on driver distraction," *Traffic Injury Prevention*, vol. 14, no. 5, pp. 469–476, 2013.
- [12] V. Ross, E. M. Jongen, W. Wang et al., "Investigating the influence of working memory capacity when driving behavior is combined with cognitive load: an lct study of young novice drivers," *Accident Analysis & Prevention*, vol. 62, pp. 377–387, 2014.
- [13] Z. G. Du, F. Huang, B. Ran, and X. D. Pan, "Safety evaluation of illuminance transition at highway tunnel portals on basis of visual load," *Transportation Research Record*, vol. 2458, pp. 1–7, 2014.
- [14] Q. Cai, M. Abdel-Aty, J. Yuan, J. Lee, and Y. Wu, "Real-time crash prediction on expressways using deep generative models," *Transportation Research Part C: Emerging Technologies*, vol. 117, Article ID 102697, 2020.
- [15] P. Konstantopoulos, P. Chapman, and D. Crundall, "Exploring the ability to identify visual search differences when observing drivers' eye movements," *Transportation Research Part F: Traffic Psychology and Behaviour*, vol. 15, no. 3, pp. 378–386, 2012.
- [16] P. J. Hills, C. Thompson, and J. M. Pake, "Detrimental effects of carryover of eye movement behaviour on hazard perception accuracy: effects of driver experience, difficulty of task, and hazardousness of road," *Transportation Research Part F: Traffic Psychology and Behaviour*, vol. 58, pp. 906–916, 2018.
- [17] D. Babić, H. Dijanić, L. Jakob, D. Babic, and E. Garcia-Garzon, "Driver eye movements in relation to unfamiliar traffic signs: an eye tracking study," *Applied Ergonomics*, vol. 89, Article ID 103191, 2020.
- [18] R. Yu, Y. Wang, Z. Zou, and L. Wang, "Convolutional neural networks with refined loss functions for the real-time crash risk analysis," *Transportation Research Part C: Emerging Technologies*, vol. 119, Article ID 102740, 2020.
- [19] Y. Q. Yang, J. Y. Chen, S. M. Easa, Z. Y. He, D. N. Yin, and X. Y. Zheng, "Internal causes of return trip effect based on eye movement and EEG indices," *Transportation Research Part F: Traffic Psychology and Behaviour*, vol. 76, pp. 286–296, 2021.
- [20] S. Y. He, B. Liang, G. B. Pan, F. Wang, and L. L. Cui, "Influence of dynamic highway tunnel lighting environment on driving safety based on eye movement parameters of the driver," *Tunnelling and Underground Space Technology*, vol. 67, pp. 52–60, 2017.
- [21] M. M. Duan, B. M. Tang, X. H. Hu, B. K. He, and T. Z. Liu, "Driver's visual load at tunnel entrance and exit of sections with high ratio of tunnels," *Journal of Transportation Systems Engineering Information Technology*, vol. 18, pp. 113–119, 2018.
- [22] F. T. Jiao, Z. G. Du, S. S. Wang, H. R. Zheng, and S. Q. Zhuo, "Visual characteristic and comfort at the entrance and exit of

- the extra-long urban underwater tunnel,” *China Journal of Highway and Transport*, vol. 33, p. 147, 2020.
- [23] Q. Meng and X. B. Qu, “Estimation of rear-end vehicle crash frequencies in urban road tunnels,” *Accident Analysis & Prevention*, vol. 48, pp. 254–263, 2012.
- [24] M. Kinateder, P. Pauli, M. Müller et al., “Human behaviour in severe tunnel accidents: effects of information and behavioural training,” *Transportation Research Part F: Traffic Psychology and Behaviour*, vol. 17, pp. 20–32, 2013.
- [25] W. Van Winsum, “A threshold model for stimulus detection in the peripheral detection task,” *Transportation Research Part F: Traffic Psychology and Behaviour*, vol. 65, pp. 485–502, 2019.
- [26] A. Mehri, M. Aliabadi, R. Golmohammadi, and S. A. Zakerian, “An empirical investigation of disability glare and visibility level during driving inside very long road tunnels: a case study,” *Tunnelling and Underground Space Technology*, vol. 125, Article ID 104496, 2022.
- [27] Y. Yang, Y. Chen, C. Wu, and S. M. Easa, “Comparative study on drivers’ eye movement characteristics and psycho-physiological reactions at tunnel entrances in plain and high-altitude areas: a pilot study,” *Tunnelling and Underground Space Technology*, vol. 122, Article ID 104370, 2022.
- [28] H. Lu, C. Zhang, L. Jiao, Y. Wei, and Y. Zhang, “Analysis on the spatial-temporal evolution of urban agglomeration resilience: a case study in Chengdu-Chongqing Urban Agglomeration, China,” *International Journal of Disaster Risk Reduction*, vol. 79, Article ID 103167, 2022.
- [29] T. Shang, H. Qi, A. Huang, and T. Liu, “A comparative driving safety study of mountainous expressway individual tunnel and tunnel group based on eye gaze behavior,” *PLoS One*, vol. 17, no. 2, Article ID e0263835, 2022.
- [30] C. Siddique and X. J. Ban, “State-dependent self-adaptive sampling (SAS) method for vehicle trajectory data,” *Transportation Research Part C: Emerging Technologies*, vol. 100, pp. 224–237, 2019.
- [31] Z. Y. Cheng, W. Wang, J. Lu, and X. Xing, “Classifying the traffic state of urban expressways: a machine-learning approach,” *Transportation Research Part A: Policy and Practice*, vol. 137, pp. 411–428, 2020.
- [32] Y. S. Li and W. J. Wang, “Research on optimal design of urban tunnel lighting,” *Journal of Chongqing Jiaotong University (Natural Science Edition)*, vol. 39, pp. 76–91, 2020.
- [33] A. Y. Chen, Y.-L. Chiu, M.-H. Hsieh, P.-W. Lin, and O. Angah, “Conflict analytics through the vehicle safety space in mixed traffic flows using UAV image sequences,” *Transportation Research Part C: Emerging Technologies*, vol. 119, Article ID 102744, 2020.
- [34] J. Wang and Q. X. Shi, “Short-term traffic speed forecasting hybrid model based on chaos-wavelet analysis-support vector machine theory,” *Transportation Research Part C: Emerging Technologies*, vol. 27, pp. 219–232, 2013.
- [35] F. Basso, L. J. Basso, F. Bravo, and R. Pezoa, “Real-time crash prediction in an urban expressway using disaggregated data,” *Transportation Research Part C: Emerging Technologies*, vol. 86, pp. 202–219, 2018.
- [36] Z. Elamrani Abou El Assad, H. Mousannif, and H. Al Moatassime, “A real-time crash prediction fusion framework: an imbalance-aware strategy for collision avoidance systems,” *Transportation Research Part C: Emerging Technologies*, vol. 118, Article ID 102708, 2020.
- [37] M. Chai, S. W. Li, W. C. Sun, M. Z. Guo, and M. Y. Huang, “Drowsiness monitoring based on steering wheel status,” *Transportation Research Part D: Transport and Environment*, vol. 66, pp. 95–103, 2019.
- [38] M. Rahman, M.-W. Kang, and P. Biswas, “Predicting time-varying, speed-varying dilemma zones using machine learning and continuous vehicle tracking,” *Transportation Research Part C: Emerging Technologies*, vol. 130, Article ID 103310, 2021.
- [39] S. Z. Feng, F. Q. Xu, W. X. Mao, and Z. G. Du, “Evaluation of sight guidance system at the entrance of expressway tunnel based on space right of way,” *Highways*, vol. 66, pp. 222–229, 2021.
- [40] F. Q. Pan, H. T. Pan, Z. W. L. X. Zhang, C. X. Ma, and J. S. Yang, “Analysis and modeling of driver’s visual characteristics at the entrance and exit of submarine tunnel under the coupling effect of illumination and longitudinal slope,” *Transportation System Engineering and Information*, vol. 21, pp. 142–148, 2021.
- [41] S. Li, G. F. Li, Y. Cheng, and B. Ran, “Urban arterial traffic status detection using cellular data without cellphone GPS information,” *Transportation Research Part C: Emerging Technologies*, vol. 114, pp. 446–462, 2020.
- [42] X. D. Pan, Y. C. Song, Z. Yang, and G. S. Zhang, “Visual environment improving scope at entrance and exit of highway tunnel based on visual load,” *Journal of Tongji University*, pp. 777–780, 2009.
- [43] M. Xu, X. D. Pan, F. Chen, and X. X. Ma, “Experimental study on the effect of color light vision regulation on hypnotic relief of long tunnel driving,” *Zhongguo Gonglu Xuebao.China Journal of Highway and Transport*, vol. 33, pp. 235–244, 2020.
- [44] Y. F. Bao, M. N. Wang, P. C. Qin, J. Y. Chen, T. Yan, and C. L. Han, “Design of awnings for highway tunnel group based on visual adaptation curve,” *Modern Tunnel Technology*, vol. 57, pp. 120–126, 2020.
- [45] D. Zhigang, Z. J. Zheng, M. Zheng, B. Ran, and X. Zhao, “Drivers’ visual comfort at highway tunnel portals: a quantitative analysis based on visual oscillation,” *Transportation Research Part D: Transport and Environment*, vol. 31, pp. 37–47, 2014.
- [46] H. Ding, Y. Lu, N. N. Sze, T. Chen, Y. Guo, and Q. Lin, “A deep generative approach for crash frequency model with heterogeneous imbalanced data,” *Analytic methods in accident research*, vol. 34, Article ID 100212, 2022.
- [47] W. Lin, X. Zheng, C. Wu, S. M. Easa, W. Lin, and X. Zheng, “Effect of highway directional signs on driver mental workload and behavior using eye movement and brain wave,” *Accident Analysis & Prevention*, vol. 146, Article ID 105705, 2020.